ORIGINAL PAPER

Interannual and spatial variation in small zooplankton off Vincennes Bay, East Antarctica

Aiko Tachibana[1] · Yuri Ohkubo[1] · Kohei Matsuno[2] · Keigo D. Takahashi[3] · Ryosuke Makabe[1,3,4] · Masato Moteki[1,4]

Abstract

Although small zooplankton are an important component of both the classical food web and microbial loop, fundamental information about small zooplankton in the Southern Ocean is lacking. This study presents the interannual and horizontal variabilities of small zooplankton and the population structure of the key small copepod species *Ctenocalanus citer* off Vincennes Bay, East Antarctica. Zooplankton were sampled with a 100 µm mesh net during austral summer from 2016 to 2018. Small copepods numerically dominated all samples, with *Oithona* spp., Oncaeidae, *C. citer* and nauplii being particularly abundant (> 75% of total zooplankton abundance). Community structure analysis revealed annual and latitudinal changes in the community, which were driven by the timing of sea-ice retreat and associated with the phytoplankton bloom. The population structure of *C. citer* showed variability not only with latitude but also between eastern and western areas. The water temperature gradient formed by cyclonic eddies likely influences the developmental period of *C. citer*, thereby generating the east–west difference in population structure. Spatial differences in the population structure of copepods attributable to cyclonic eddies are likely common during summer in East Antarctica. Our results demonstrate that the development of *C. citer* population structure is synchronised with short-term fluctuations in phytoplankton size composition following sea-ice retreat, suggesting that the phytoplankton bloom is efficiently used for population growth in the seasonal ice zone. These data suggest that small zooplankton respond rapidly to local environmental changes.

Keywords *Ctenocalanus citer* · Phytoplankton bloom · Sea-ice retreat · Small zooplankton · Vincennes eddy

Introduction

Small copepods (< 1.5 mm) are abundant in the zooplankton community and are important links in marine food webs (Turner 2004). Nevertheless, most research on zooplankton abundance and distribution has been based on net samples, in which the mesh sizes are often too coarse to capture small copepods (≥ 200 µm). Hence, this group is significantly underestimated in most current and historical datasets (Gallienne and Robins 2001; Turner 2004; Pansera et al. 2014). In the Southern Ocean, small cyclopoid (*Oithona*, Oncaeidae) and calanoid (*Clausocalanus*, *Microcalanus*) copepods, as well as juvenile forms of larger copepods, are abundant in the micro- and meso-sized zooplankton communities (Hopkins and Torres 1988; Schnack-Schiel et al. 2008; Stevens et al. 2015; Ojima et al. 2015; Takahashi et al. 2017; Makabe et al. 2017), although fine-mesh plankton nets (100–200 µm mesh size) have rarely been used to study the zooplankton community.

Small zooplankton link lower and higher trophic levels via both the microbial loop and the classical food chain (Turner 1984; Atkinson 1998). Feeding by small copepod species on the phytoplankton, protozoans and zooplankton within the epipelagic layers of the Southern Ocean controls lower trophic levels and carbon uptake efficiency (Atkinson 1996; Dubischar et al. 2002; Smetacek et al. 2004; Halfter

✉ Aiko Tachibana
   atachi0@kaiyodai.ac.jp

1 Department of Ocean Sciences, Tokyo University of Marine Science and Technology, 4-5-7 Konan, Minato, Tokyo 108-8477, Japan

2 Faculty/Graduate School of Fisheries Sciences, Hokkaido University, 3−1−1 Minato-Cho, Hakodate, Hokkaido 041-8611, Japan

3 Department of Polar Science, Graduate University for Advanced Studies, SOKENDAI, 10-3 Midori-Cho, Tachikawa, Tokyo 190-8518, Japan

4 National Institute of Polar Research, 10-3 Midori-Cho, Tachikawa, Tokyo 190-8518, Japan

et al. 2020). In addition, zooplankton respond rapidly to environmental change, and their community structure and abundance are influenced by organisms at higher trophic levels through the food chain (Atkinson et al. 2012). Therefore, investigating the zooplankton community, including small copepods, is essential for elucidating the ecosystems and biogeochemical cycles in the Southern Ocean.

Ecosystem dynamics in the seasonal ice zone (SIZ) are driven by the Antarctic Circumpolar Current (ACC) and related frontal systems, as well as the annual advance and retreat of sea ice (Hunt and Hosie 2005; Massom and Stammerjohn 2010; Nicol and Raymond 2012). The macro-zooplankton community, including krill and large copepods, changes with the position of these frontal systems (Hunt et al. 2007; Ward et al. 2012b; Tachibana et al. 2017). In particular, the distribution patterns of some large zooplankton species are affected by the position of the southern boundary (SB) of the ACC (Hunt et al. 2007; Tanimura et al. 2008). Small zooplankton communities are affected by sea-ice dynamics associated with the seasonal phytoplankton bloom (Takahashi et al. 2017; Makabe et al. 2017). Higher primary production at sea-ice edges (ice-edge blooms) observed during sea-ice retreat in spring and summer generally affects the development of small copepods, such as *Ctenocalanus citer* and *Oithona similis* (Atkinson 1998). The timing of sea-ice melting and the occurrence of phytoplankton blooms vary interannually and are subject to climate change (Montes-Hugo et al. 2009; Stammerjohn et al. 2012; Rohr et al. 2017). However, information about the interannual variability of the small zooplankton community related to sea-ice dynamics is scarce.

Among the small zooplankton communities in the Southern Ocean, *C. citer* is a common species distributed in the upper 200 m during summer (e.g. Schnack-Schiel and Mizdalski 1994; Schnack-Schiel 2001). The reproductive period begins in early spring, and the seasonal vertical migration occurs during the spring–summer transition (Schnack-Schiel and Mizdalski 1994). Although regional differences in the timing of their seasonal ascent behaviour are observed off Lützow-Holm Bay in the Indian Ocean sector during summer, the factors affecting these differences have not been elucidated (Makabe et al. 2017). Furthermore, the relationship between phytoplankton abundance by the size fraction and distribution of *C. citer*, which prefers smaller (< 10 μm) phytoplankton (Pasternak and Schnack-Schiel 2007) is less documented. Information on the spatial variability of the population structure and vertical distribution in relation to environmental factors, including prey size composition, are limited, although this species is potentially important in the Southern Ocean ecosystem.

We conducted transect observations in January 2016–2018 in the SIZ along the 110°E meridian off Vincennes Bay, East Antarctica (Fig. 1). The transect is spanned by major fronts, namely, the SB of the ACC and the Southern ACC Front (SACCF). In addition, a series of cyclonic eddies occurs off Wilkes Land, East Antarctica (Mizobata et al. 2020). This eddy circulation transports warm circumpolar deep water (CDW) poleward on the eastern side of the eddy, and transports cold water equatorward on the western side (Mizobata et al. 2020). This means that this physical process forms, not only north–south, but also east–west water temperature gradients in the water where the eddy is located. Characteristics of these local oceanographic circulation patterns may influence the small copepod community and its population structure; however, little is yet known about the effects of these local hydrographic structures. This study investigated the annual and spatial variation in community structure of small zooplankton in the SIZ to clarify the influence of local eddies and sea-ice dynamics on that community. In addition, for the key small calanoid copepod *C. citer*, environmental variables, including the influence of local eddies, were examined to explain the spatial variation in their population structures, providing information about the life cycle strategies of copepods in the Southern Ocean.

Materials and methods

Field sampling and environmental data collection

Zooplankton were sampled from a transect along 110°E in the SIZ off Vincennes Bay during three voyages each January from 2016 to 2018 aboard the training vessel *Umitaka-maru* of the Tokyo University of Marine Science and Technology (Fig. 1). During the 2016 voyage, vertical tows from 200 to 0 m depth at a speed of approximately 1 m s^{-1} using a Norpac net (100 μm mesh size, 45 cm mouth diameter) with an attached flow meter (Rigo Co. Ltd.) were conducted. For sampling in 2017 and 2018, a vertical multiple plankton sampler (VMPS, Tsurumi-Seiki Co. Ltd.) with a 0.25 m^2 mouth area and 100 μm mesh was used. Discrete depth samples were collected from three (200–100, 100–50, 50–0 m) or four layers (200–150, 150–100, 100–50, 50–0 m) using a multiple-net opening/closing system at a speed of approximately 1 m s^{-1} (Table 1). The filtered volume was determined using a digital flow meter installed on the net system. In 2017, a latitudinal transect of seven stations along 63.5°S, crossing the Vincennes eddies, was sampled to investigate the interactions of zooplankton community structure with oceanographic conditions. Hydrographic information, particularly regarding eddies in 2017 along the latitudinal transect, was described by (Mizobata et al. 2020). A total of 21 zooplankton samples (including six samples using a Norpac net in 2016 and 15 samples using a VMPS in 2017 and 2018) were collected and immediately preserved with buffered 5% formaldehyde and seawater solution. Although the net mouth

Fig. 1 Zooplankton sampling locations off Vincennes Bay, East Antarctica, in January from 2016 to 2018. **a** Overall view of Antarctica, with extent of image **b** indicated by blue square. **b** Map of the study area. Legends (pulses, red circles and blue triangles) indicate the sampling location in each year. Green x indicates CTD stations. Circulation arrows denote the Vincennes eddy, drawn with reference to Mizobata et al. (2020)
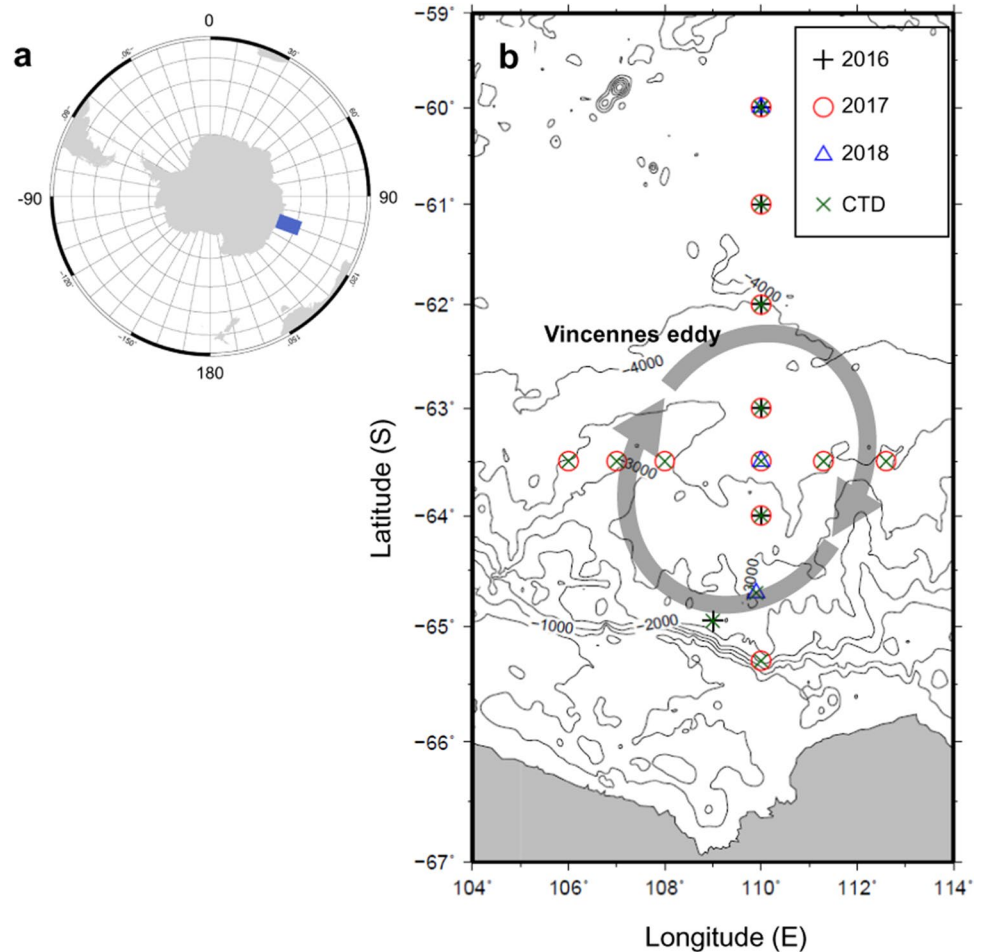
area was slightly larger in the latter between the Norpac net and the VMPS (0.16 vs. 0.25 m², respectively), we assumed that there was no difference in net avoidance of small zooplankton because the same mesh size (100 μm) and towing speed were used. Therefore, we considered that biases due to differences in sampling methods would be negligible, and used the data collected by the Norpac net and the VMPS together in the analysis of interannual variability of the small zooplankton community. Additional information is provided in Online Resources 1 and 2.

Vertical temperature and salinity profiles were obtained using a conductivity, temperature and depth profiler system (CTD; SBE 9plus, Sea-Bird Electronics, Bellevue, WA, USA) at all sampling stations. Detailed information on the CTD data is available in the reports of the Polar Data Journal (Shimada et al. 2020) and the Polar Science Data Archives (JARE57; http://polaris.nipr.ac.jp/~parc/usr/di_list.php?pid=271). The Southern Ocean is characterised by the ACC, which separates different water masses (Orsi et al. 1995). The positions of the oceanic fronts were determined from an underwater environmental monitoring system (ETSG 2 Thermosalinograph, Falmouth Scientific, Inc., Procasset,

MA, USA) in combination with the CTD data, following the definitions of (Orsi et al. 1995) and (Sokolov and Rintoul 2002). We defined the region north of the northern branch of the Southern ACC front (SACCF-N) as the Northern Antarctic Zone (AZN), the region between the SACCF-N and the southern boundary of the ACC as the Southern Antarctic Zone (AZS) and the region south of the southern boundary of the ACC as the SB, according to (Hunt and Hosie 2005). The surface mixed layer depth (MLD) at each location was determined according to the criteria of (Aoki et al. 2006).

Water samples were collected with a CTD multi-bottle rosette sampler equipped with 24 12-L Niskin bottles (General Oceanics, Miami, FL, USA) at all sampling stations and then filtered through membrane filters (pore sizes 10 and 2 μm) and onto grass-fibre filters (Whatman GF/F) to obtain > 10 (Chl_10), 2–10 (Chl_2) and < 2 μm (GF/F) size fractions, respectively. Chlorophyll *a* (chl *a*) was extracted with *N*,*N*-dimethylformamide (Suzuki and Ishimaru 1990), and its concentration was determined using a Turner fluorometer (AU-10, Turner Designs, San Jose, CA, USA). Detailed information on chl *a* is available in the reports of the Polar Data Journal (Makabe et al. 2019, 2020). Ice-free

Table 1 List of sampling locations and their environment information

Sample name	Station	Data (UTC)	Latitude (S)	Longitude (E)	Zone	Temp200	Sal200	Size-fractionated chlorophyll *a* of surface			MLD	IFD	Gear	Layer
								Chl_10	Chl_2	GF/F				
16_60S	KC5	23-01-2016	60.000	110.002	AZN	0.61	33.7	0.66	0.17	0.05	69	93	NORPAC	0-200
16_61S	C02	24-01-2016	61.000	110.002	AZS	0.74	33.6	0.34	0.15	0.04	55	112	NORPAC	0-200
16_62S	C03	25-01-2016	62.000	110.001	AZS	0.59	33.3	0.23	0.20	0.04	48	83	NORPAC	0-200
16_63S	C04	25-01-2016	63.001	109.993	AZS	0.65	33.5	0.55	0.17	0.07	41	77	NORPAC	0-200
16_64S	C05	26-01-2016	64.000	109.998	SB	0.03	33.4	1.37	0.21	0.04	30	45	NORPAC	0-200
16_65S	KC6	27-01-2016	64.973	109.018	SB	− 1.69	32.9	0.92	0.66	0.10	26	21	NORPAC	0-200
17_60S	KC5	07-01-2017	59.999	110.005	AZN	0.80	33.7	0.06	0.05	0.02	41	97	VMPS	0-50-100-200
17_61S	KM4	08-01-2017	60.996	110.005	AZN	0.37	33.7	0.05	0.05	0.03	36	62	VMPS	0-50-100-200
17_62S	C03	09-01-2017	62.000	110.001	AZS	0.49	33.7	0.09	0.06	0.03	29	63	VMPS	0-50-100-200
17_63S	C05	16-01-2017	63.000	109.996	AZS	0.52	33.5	0.04	0.04	0.03	40	66	VMPS	0-50-100-150-200
17_63.5S110E	C06	17-01-2017	63.475	109.980	AZS	0.43	33.6	0.05	0.05	0.03	39	67	VMPS	0-50-100-150-200
17_64S	C07	10-01-2017	64.250	109.999	SB	− 0.50	33.9	0.59	0.01	0.16	51	51	VMPS	0-50-100-200
17_65.5S	KC6	11-01-2017	65.284	109.998	SB	− 1.13	33.7	0.10	0.13	0.05	30	0	VMPS	0-50-100-200
17_106E	C09	13-01-2017	63.493	105.966	SB	− 0.35	33.6	0.06	0.05	0.02	38	51	VMPS	0-50-100-200
17_107E	C10	14-01-2017	63.498	106.996	SB	− 0.61	33.6	0.08	0.07	0.04	30	54	VMPS	0-50-100-200
17_108E	C11	15-01-2017	63.500	107.997	SB	− 0.88	33.7	0.04	0.08	0.06	36	61	VMPS	0-50-100-200
17_111E	C14	18-01-2017	63.500	111.329	AZS	0.89	33.7	0.05	0.04	0.02	38	62	VMPS	0-50-100-150-200
17_112E	C15	19-01-2017	63.500	112.662	AZS	0.66	33.6	0.08	0.05	0.03	38	63	VMPS	0-50-100-150-200
18_60S	KC5	08-01-2018	59.999	110.000	AZN	0.62	33.6	0.66	0.11	0.03	47	98	VMPS	0-50-100-150-200
18_63.5S	B01	10-01-2018	63.498	110.049	AZS	0.56	33.6	0.15	0.02	0.25	34	44	VMPS	0-50-100-150-200
18_65S	KC6	11-01-2018	64.690	109.877	SB	− 1.56	33.1	0.09	0.36	0.05	12	29	VMPS	0-50-100-150-200

AZN Northern Antarctic Zone, which was located north of the northern branch of the Southern ACC front (SACCF-N); *AZS* Southern Antarctic Zone, which was located between the SACCF-N, the southern boundary of the ACC; *SB* South of the Southern Boundary, Temp200 = Average water temperature from 0 to 200 m, Sal200 = Average water salinity from 0 to 200 m, Chl_10 = > 10 μm chlorophyll a concentration, Chl_2 = 10–2 μm chlorophyll a concentration, GF/F = <2 μm chlorophyll a concentration, MLD = surface mixed layer depth (m) and IFD = Ice-free days at each location was defined as the number of days after the sea-ice concentration became less than 20%

days (IFDs) at each location were defined as the number of days after the sea-ice concentration (SIC) became less than 20%. Daily SIC data were determined using a bootstrap algorithm (Comiso et al. 1984; Comiso 1986) from the Advanced Microwave Scanning Radiometer 2 (AMSR2), obtained from the Japan Aerospace Exploration Agency website (http://suzaku.eorc.jaxa.jp/GCOM_W/data/data_w_use.html). Daily mean SIC data were mapped on a polar stereographic grid with a spatial resolution of 10 km and a $0.1° \times 0.1°$ Mercator grid.

Laboratory procedures

All zooplankton samples were split into two aliquots using a Motoda plankton splitter (Motoda 1959) in the laboratory, one of which was used for further analysis. Large specimens ($\geq$ 1.5 mm total length, i.e. *Calanoides acutus*, *Calanus propinquus*, *Calanus simillimus*, *Metridia gerlachei*, *Metridia lucens*, *Rhincalanus gigas* and other large zooplankton; Cnidaria, Amphipoda, Ostracoda, Euphausiacea, Polychaeta, Chaetognatha, Pteropoda and Appendicularia) were identified and counted under a stereomicroscope in one sub-sample. The sub-sample in which large specimens were excluded was further subdivided and at least 200 individuals of small specimens (< 1.5 mm) were counted and identified under a stereomicroscope (SMZ18, Nikon, Tokyo, Japan) and upright microscope (80 IE, Nikon, Tokyo, Japan). All calanoid copepods were identified to the lowest possible taxonomic level (generally species or genus), and then their developmental stages were determined under a stereomicroscope. The first copepodite (CI) stages of *C. acutus* and *C. propinquus* were combined. The older copepodite (> CIII) stages of Clausocalanidae (including *C. citer*, *Clausocalanus laticeps* and *Clausocalanus brevipes*) except for *Microcalanus pygmaeus* were highly dominated by *C. citer* (96%); therefore, we presumed that stages CI–CIII of Clausocalanidae were *C. citer* in further analysis. *M. pygmaeus* was identified to all copepodite stages. Cyclopoids and poecilostomatoids (genus *Oithona* and family Oncaeidae) were identified to the genus or family level. Other zooplankton (Cnidaria, Amphipoda, Ostracoda, Euphausiacea, Polychaeta, Chaetognatha, Pteropoda and Appendicularia) were not identified to the species level. Abundance was calculated as the number of individuals per m^3 (Online Resource 3).

Data analysis

Cluster analysis was employed using 3 years of data to elucidate interannual and spatial variation in the SIZ zooplankton community structure. The zooplankton data from 2017 and 2018 were converted to an integrated average abundance of 0–200 m (ind. m^{-3}) for comparison with 2016. The Bray–Curtis similarity and unweighted paired-group

average linkage indices were used for these analyses (Field et al. 1982). Abundance data for each taxon were root transformed before the cluster analysis to reduce the effect of underestimating large zooplankton due to net avoidance. Subsequently, permutational analysis of variance (PERMANOVA) and pairwise comparisons were conducted to identify differences among the clustered groups. PERMANOVA was conducted using type III sums of squares and the unrestricted model. Similarity percentage analysis (SIMPER) was performed to quantify the contribution of a species to the dissimilarity among the clustered groups. The environmental variables explaining the zooplankton community were analysed using the distance-based linear model permutation test (distLM). The best models were selected through a stepwise selection procedure based on the Akaike information criterion (AICc) with a correction for small sample size. The environmental factors included average water temperature (0–200 m; Temp200), average water salinity (0–200 m; Sal200), photosynthetically active radiation (PAR), size-fractionated chl *a* concentrations (Chl_10, Chl_2, GF/F) on the surface, MLD and IFDs. We measured chl *a* via water sampling in nine layers primarily from the surface to 200 m, including the subsurface chl *a* maxima (SCM), although data from several sampling layers in 2016 were lost due to sampling error. Because the surface chl *a* values were significantly correlated with the integrated chl *a* values from 0 to 200 m depth ($r = 0.906–0.840$, $p < 0.0001$), we used the surface chl *a* values as representative in the water column (to 200 m depth) for the environmental factors in the zooplankton community analysis. To remove multicollinearity between environmental parameters, variance inflation factors (VIFs) were calculated for each parameter. If the VIF exceeded 6, it was removed from the explanatory parameters. This is well below the suggested threshold of 10, indicating that the correlation between variables is low and that the parameters can be interpreted individually (O'brien 2007). Community analyses were conducted using PRIMER software version 7 with the PERMANOVA + add-on (Anderson et al. 2008; Clarke and Gorley 2015). All permutation-based tests were conducted using 999 permutations. Differences in mean abundance between groups were tested by one-way analysis of variance, and the Tukey–Kramer post hoc test was used to distinguish differences between the groups.

The effects of environmental parameters on the population structure of *C. citer* were investigated using canonical correspondence analysis (CCA) for the untransformed proportions of each developmental stage (CI–CVI) at each station in 2017 and 2018, along with normalised environmental variables. The 2016 samples were not stratified and were excluded from this analysis. The environmental variables used were the same as those in the previous section (except for surface chl *a*), with the addition of the mean

value of the size-fractionated chl *a* concentrations (Chl_10, Chl_2, GF/F). The optimal subset of variables identified by the model was selected using forward selection for adjusted R^2 values as the selection criterion. This analysis was run using the cca and ordiR2step functions of the R package vegan (Oksanen et al. 2019; R Core Team 2020). The significance of the model was analysed through permutation testing (permutations = 999) at a significance level of $p < 0.010$.

Results

Hydrography

The water mass distributions along the 110°E transect were generally similar in all 3 years. Fresher water spread along the surface mixed layer from the surface to approximately 30–50 m depth across the entire study area, reflecting the melting of sea ice (Fig. 2). Subsurface temperature minimum layers were observed below the mixed layer. Relatively warm, saline layers were found below the temperature minimum layer and identified as CDW. Along the 63.5°S transect, CDW was located in the eastern area
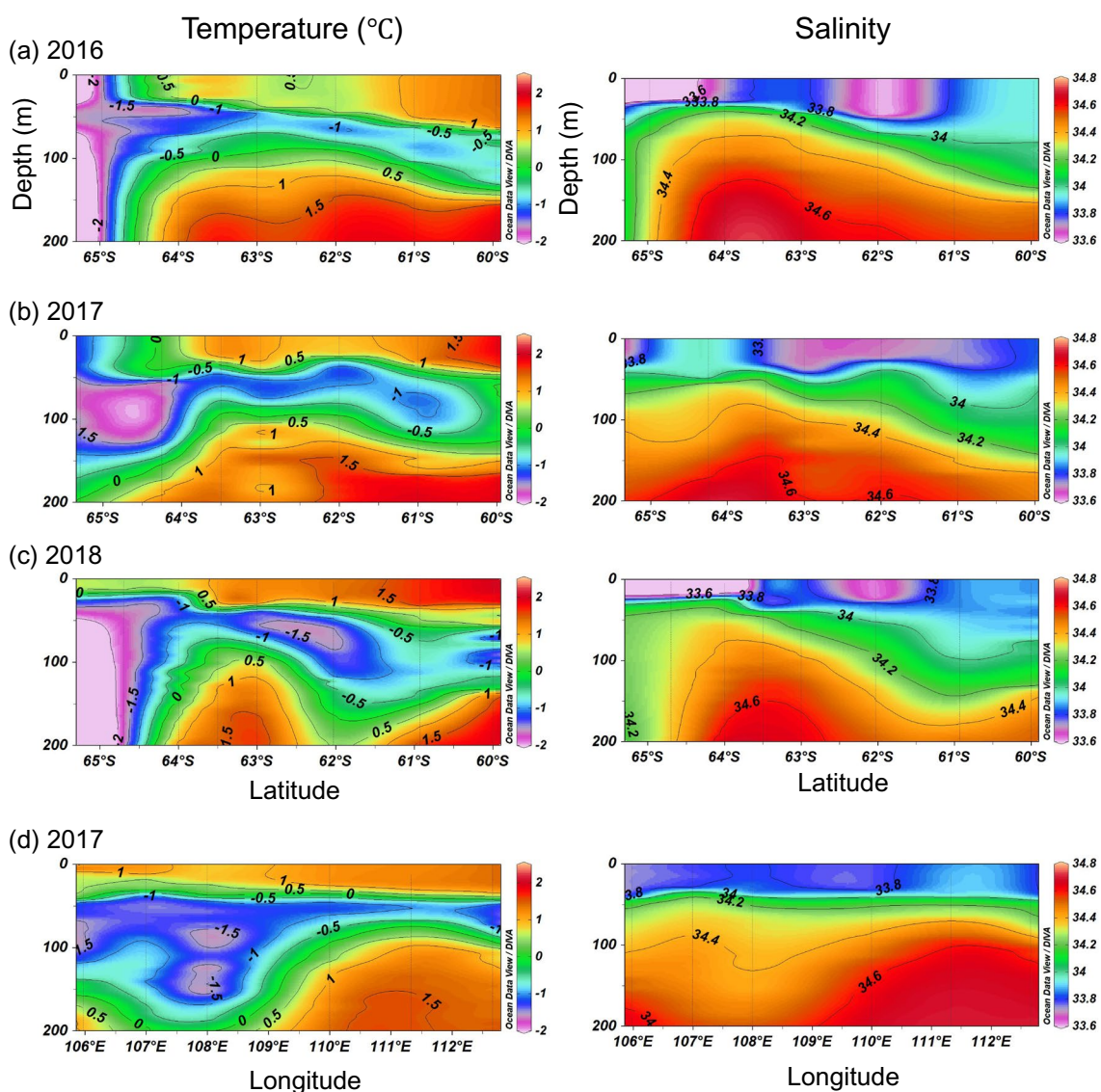
Fig. 2 Temperature and salinity contours in January of 2016 to 2018 along the 110°E (**a–c**) and 63.5°S (**d**) transect lines off Vincennes Bay, East Antarctica. SACCF-N denotes the northern branch of the Southern ACC front. SB indicates the southern boundary of the ACC

below about 100 m depth, while cold water occurred at these depths in the western area. This environmental gradient formed due to the Vincennes eddy (Fig. 1; (Mizobata et al. 2020). SACCF-N was identified between 60° and 62° S (Table 1). SB was located between 63.5° and 64°S every year along the 110°E transect. The MLD varied with latitude, with the deepest value each year observed at the northernmost station (Table 1). The number of IFDs was slightly higher in the eastern area than on the western side,

and was also higher in 2016 than the other 2 years, likely because the survey was conducted about 2 weeks later.

The chl *a* concentration of each size fraction varied according to year and location (Table 1 and Fig. 3). Surface chl *a* concentrations in the larger two size fractions (Chl_10 and Chl_2) were higher at the southern stations (64 and 64.5°S) in 2016 than in the other 2 years (Table 1). At the northernmost station (60°S), the chl *a* concentration of the largest fraction (Chl_10) was relatively high in all years. The chl *a* concentration of the smallest fraction

Fig. 3 Vertical distribution of the chlorophyll *a* concentration in various size fractions of 2016 to 2018 along the 110°E and 63.5°S transect lines. **a**: 110°E transect in 2016, **b**: 110°E transect in 2016, **c**: 63.5°S transect in 2017 and **d**: 110°E transect in 2018. The dashed lines indicate the zooplankton sampling layer
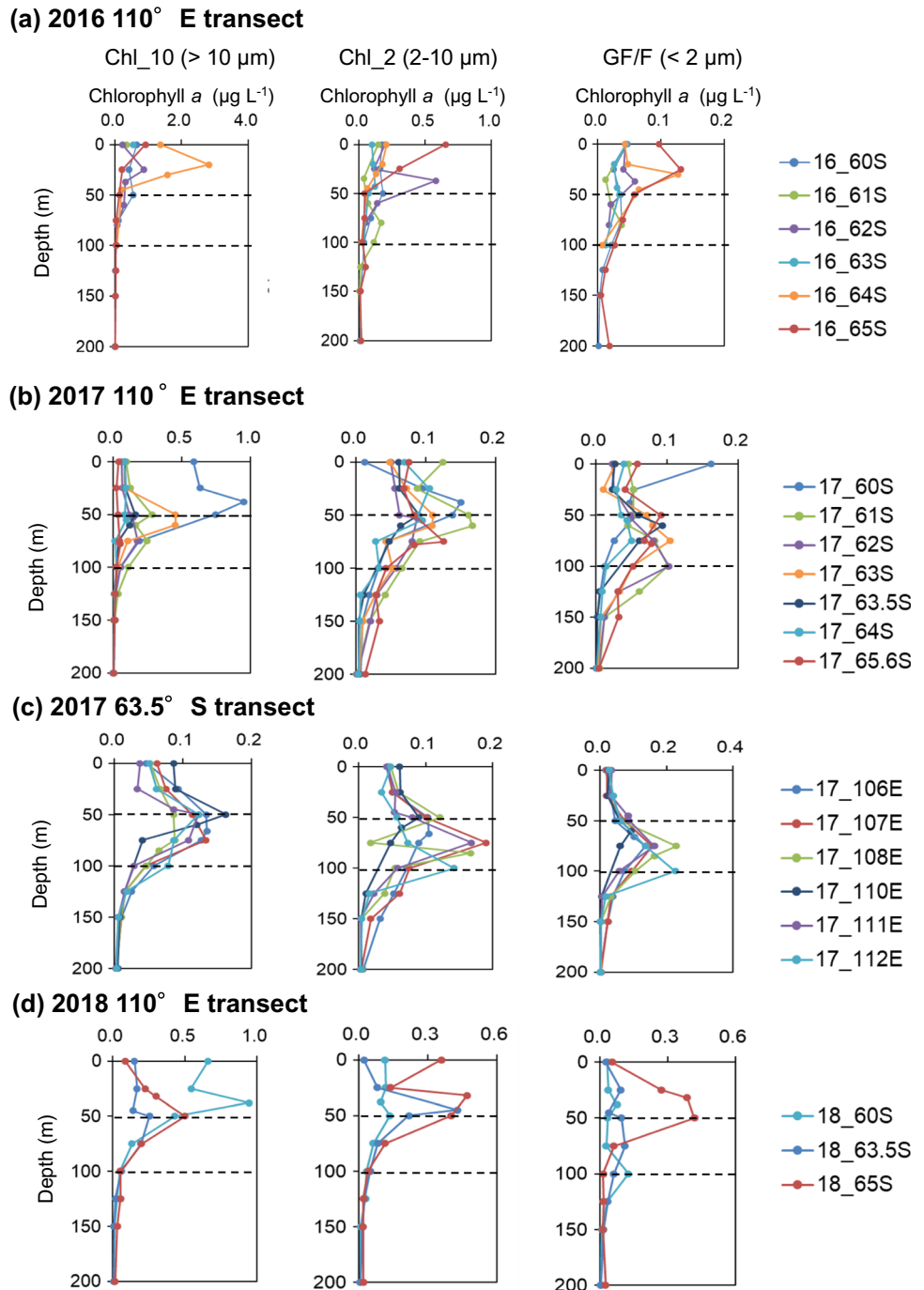
(GF/F size fraction) was highest at 63.5°S in 2018. Along the 63.5°S transect in 2017, chl *a* concentration in all size fractions were less than 0.1 µg L^{-1} throughout the transect, and spatial variation was lower than along the 110° E transect. The SCM varied latitudinally (Fig. 3). In the two size fractions, Chl_10 and Chl_2, in 2017 and the large size fraction, Chl_10, in 2018, SCM were shallower in the north (< 50 m) and deeper in the south (50–100 m). The size fractions, Chl_2 and GF/F, in 2018 were shallower at the southern station (65°S) than those at northern stations. Along the 63.5°S transect in 2017, SCM were observed at depths of 50–100 m, with fewer differences between stations. In the latitudinal and longitudinal transects, SCM depths tended to be shallow in the larger fractions.

Abundance and species composition of zooplankton

Summarising the 3 years, the total zooplankton abundance ranged from 236 to 16,429 ind. m^{-3}, with the lowest abundance in the southern area along 110°E, which was located in the SB area, while the highest abundance was observed at the northernmost station (AZN) in each year. The abundance was much lower along both 110°E and 63.5°S transects in 2017 than in other years (Fig. 4a, b). Copepods, including nauplii, were dominant at all stations, accounting for 81–99% of total zooplankton abundance (Fig. 4a, b). The relative abundance of copepod nauplii was higher in the southern area, with a maximum of 53% of the total abundance at 63°S. Appendicularia were abundant around 63–64°S. Other plankton, including Polychaeta, Pteropoda, Chaetognatha, Ostracoda, Cnidaria, Euphausiacea and

Fig. 4 Horizontal variation in total zooplankton and copepod abundances and compositions in January of 2016 to 2018 along the 110°E (**a**, **c**) and 63.5°S (**b**, **d**) transect lines off Vincennes Bay, East Antarctica
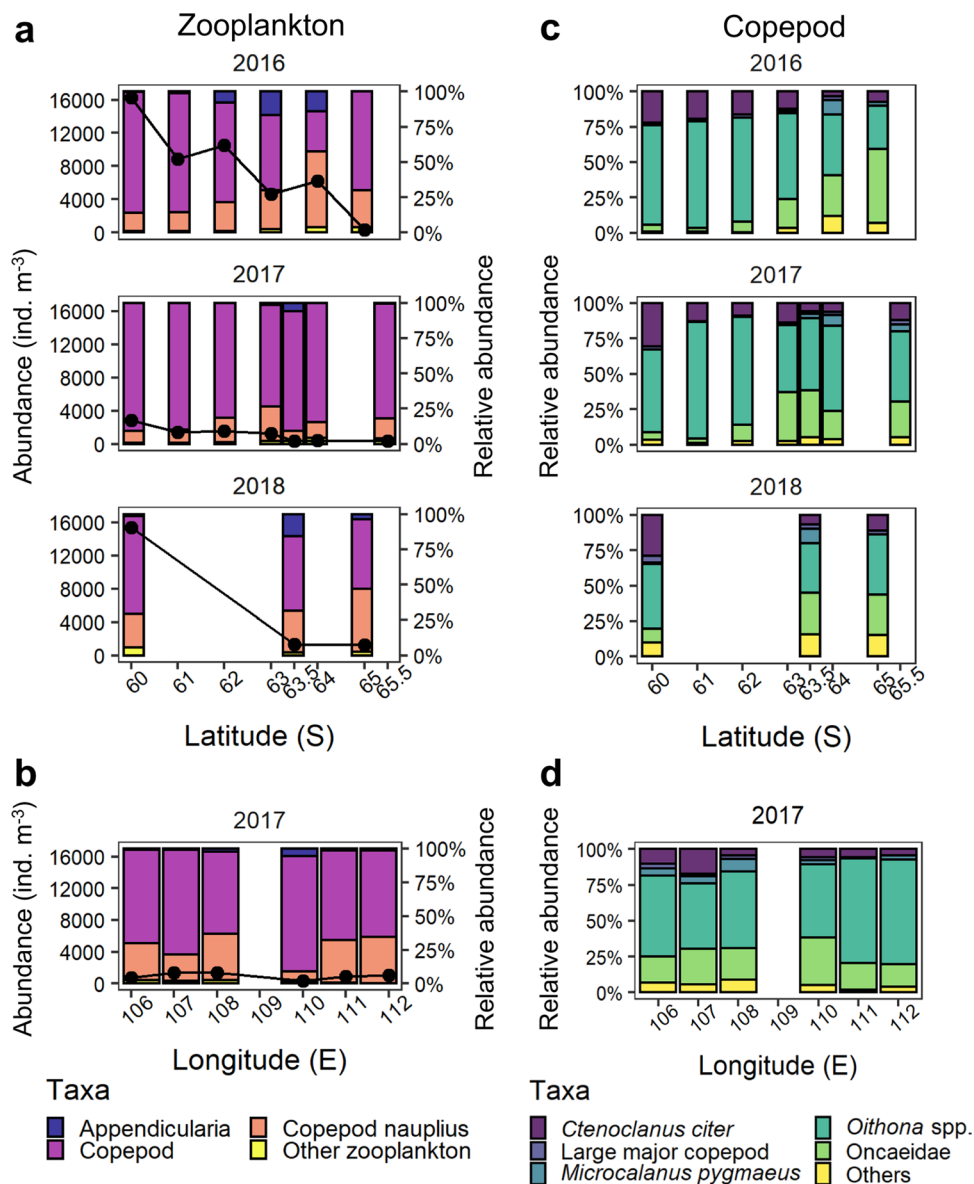
Amphipoda, accounted for a maximum of approximately 6% of the total abundance.

Along the 110°E transect, *Oithona* spp. was the predominant copepod taxon throughout the survey area (30.7–82.2%, Figs. 4c, d); in particular, high abundances were recorded at the northern stations. Oncaeidae were the second most abundant copepod at southern stations (south of 63°S, 2.5–52.0%). *C. citer* occurred throughout the survey area. *Microcalanus pygmaeus* occurred south of 63°S. Large copepods were observed at low abundances of less than 5% at all sampling stations. *Oithona* spp. was the dominant taxon along the 63.5°S transect, followed by Oncaeidae *C. citer* and *M. pygmaeus* were more dominant west of 110°E.

At the northernmost station, *Oithona* spp. was most abundant at 0–50 m depth among all depth layers in 2017. At other stations, it was found mainly at 50–100 m, although the differences among layers were smaller at 63.5°S (Fig. 5a). A similar pattern was observed in 2018 (Fig. 5c). Along the 63.5°S transect, *Oithona* spp. was distributed in the 50–100 m layer, except at 110°E (Fig. 5b). Although Oncaeidae were abundantly distributed in the 0–100 m layers at 60°S in both 2017 and 2018 (Fig. 5a, c), this taxon was less abundant in the surface layer (0–50 m) at other stations and was distributed mainly at 50–200 m along the 110°E transect and at eastern stations along the 63.5°S transect (Fig. 5a, b). At the western four stations, higher abundances were recorded in the deeper layer of 100–200 m. The distribution pattern of *C. citer* showed a higher abundance in the shallowest layer (0–50 m) only at 60°S, while at stations south of 60°S, higher abundances were apparent at 50–200 m (Fig. 5a). This distribution pattern corresponds to that observed in 2018 (Fig. 5c). No east–west trend in the surface layer (0–50 m) was found along 63.5°S transect, although this species was distributed in the 50–200 m layer throughout the transect (Fig. 5b).

Statistical analyses of the small zooplankton community

The overall zooplankton community was divided into one sample (B; 65°S in 2016) and three groups (A, C and D) at 65% similarity through cluster analysis based on the root-transformed zooplankton abundances of each sample (Fig. 6a; PERMANOVA: $p < 0.001$). The one sample (B) was characterised by very low abundance and low diversity (Fig. 6b). Clear annual differences were observed between 2016 and 2017. In addition, latitudinal changes were observed for 2017 samples between groups C (60–62°S) and D (63–65.5°S and 63.5°S transect). The 2018 samples were separated into two groups. The northernmost station was placed in group A, consisting of the 2016 group, and the remaining two stations were in group D. The abundance of group A was significantly higher than groups C and D
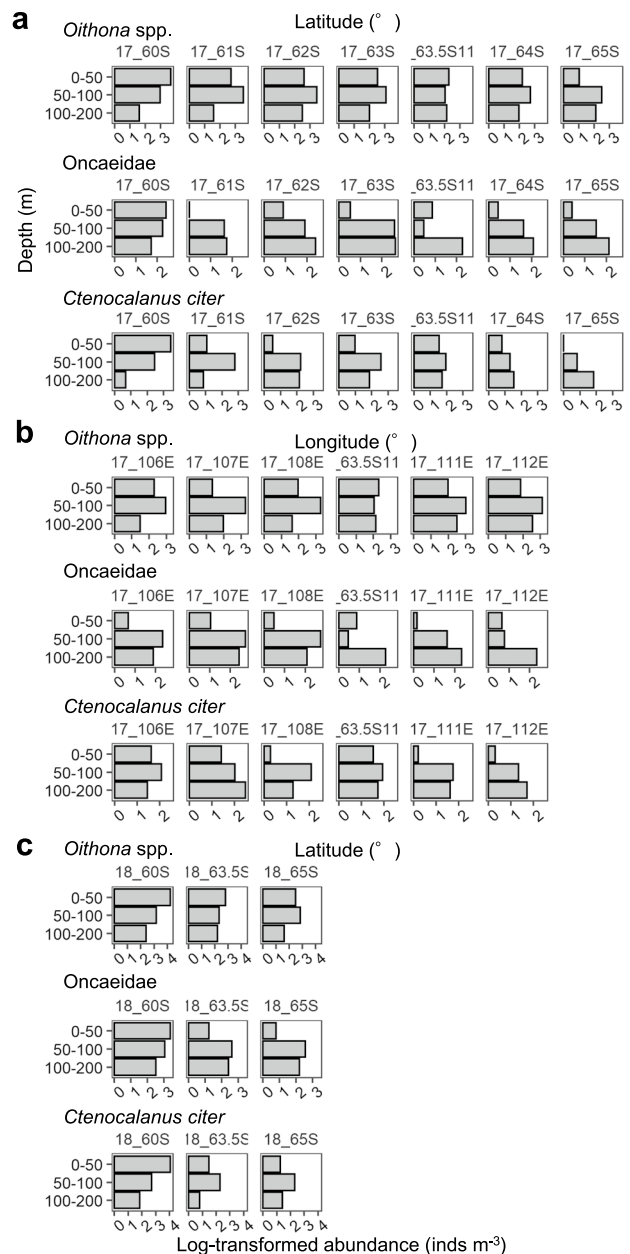
Fig. 5 Vertical distributions of three major copepod taxa (*Oithona* spp., Oncaeidae and *Ctenocalanus citer*) in the upper 200 m along the 110°E (**a**) and 63.5°S (**b**) transect lines in January 2017 and along the 110°E transect line in January 2018 (**c**) off Vincennes Bay, East Antarctica

($p < 0.0001$). Small copepods, including *Oithona* spp., nauplii and *C. citer*, were important contributors to the total abundance of each group (Fig. 6b). *Oithona* spp., *C. citer* and copepod nauplii had a high contribution in average dissimilarity in all comparisons between groups (Table 2). The average abundance of these taxa and Appendicularia was higher in group A than in groups C or D ($p = 0.024$ and 0.004, respectively). The taxa contributing to the
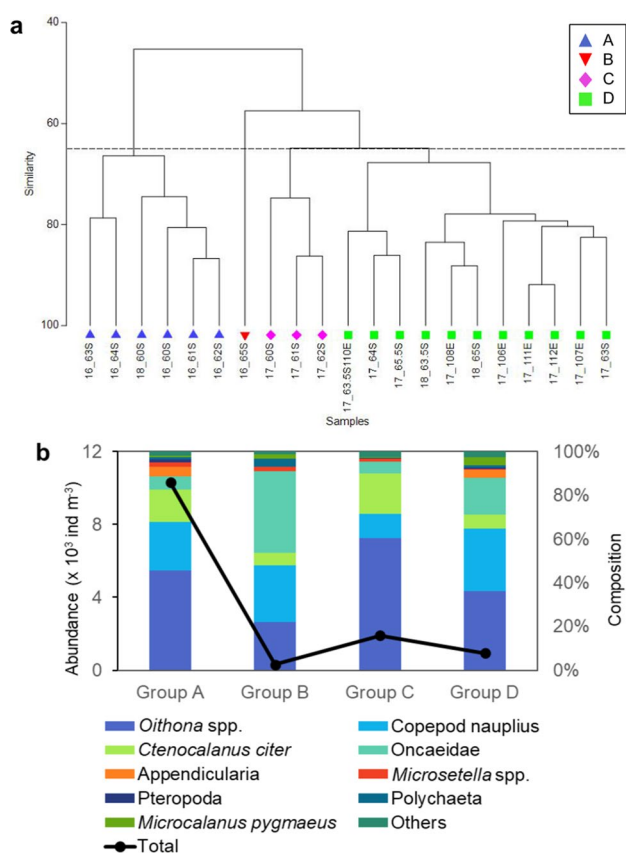
Fig. 6 Results of cluster analysis. **a**: Dendrogram based on abundances of the zooplankton community over 3 years. Each group was tested with PERMANOVA. **b**: Abundance and species composition of each group identified in cluster analysis

dissimilarity between groups C and D were small copepods of *M. pygmaeus*, *Oithona* spp. and *C. citer*. The first species was more abundant in group D, while the latter two species were much more abundant in group C. The best model of environmental factors describing the zooplankton community included IFDs ($p = 0.001$) and chl a concentration of the largest fraction (Chl_10, $p = 0.007$; Table 3). IFD and large Chl_10 were factors explaining 34.0 and 12.9% of the variation in the zooplankton community, respectively.

Population structure of *Ctenocalanus citer* and its environmental drivers

The vertical distributions of each developmental stage of *C. citer* differed spatially (Fig. 7), with *C. citer* being distributed in the surface layer in the north and in the deeper layers towards the south. Along the 110°E transect, the highest abundances of copepodite stages CI–CIV were observed in the upper 50 m at 60°S (Fig. 7a). At 61°S–63°S, early life stages (CI–CII) occurred in the 50–100 m layer at high abundances. South of 63°S, these populations were concentrated in layers deeper than 50 m. Males were found in the 50–100 m and 100–200 m layers at 60°S and 64°S, respectively, at low abundances. In 2018, high abundances of all stages except adult males were observed in the upper 50 m at 60°S (Fig. 7c). At 63.5°S and 65°S, early stages (CI–CIII) occurred in deeper layers of 50–200 m, while no trends were observed for middle stages (CIV and CV) and adult females. Along the 63.5°S transect, a high abundance of adult females was observed in the 50–100 m layer of western stations (106°E–108°E; Fig. 7b). Other stages also occurred, mainly at 50–100 m. Adult males occurred only at 100–200 m throughout the transect. There were no clear

Table 2 Species abundance (root) and their contributions as average dissimilarities (Av. Dis) to the overall average dissimilarity between each pair of groups, as indicated by the SIMPER analysis

Taxa/ Species	Average abundance		Av. Dis	% Contribution	Cumulative %
Average dissimilarity = 48.68	**Group A**	**Group C**			
Copepod nauplius	46.8	14.3	9.0	18.5	18.5
Oithona spp.	64.4	33.8	8.5	17.5	36.1
Ctenocalanus citer	35.1	17.1	5.8	12.0	48.0
Appendicularia	19.2	1.7	5.3	10.8	58.8
Average dissimilarity = 54.82	**Group A**	**Group D**			
Oithona spp.	64.4	18.1	13.4	24.4	24.4
Copepod nauplius	46.8	15.3	9.4	17.2	41.6
Ctenocalanus citer	35.1	7.3	7.8	14.2	55.8
Average dissimilarity = 35.11	**Group C**	**Group D**			
Oithona spp.	33.8	18.1	8.6	24.5	24.5
Ctenocalanus citer	17.1	7.3	5.1	14.6	39.1
Copepod nauplius	14.3	15.3	3.2	9.0	48.1
Microcalanus pygmaeus	0.7	5.5	2.5	7.0	55.1

Species contributing to the first 50% of the dissimilarity are shown in decreasing order of percentage contribution

Table 3 Results of distance-based linear model (DistLM) analyses on the relation of environmental variables to the community structure (Bray–Curtis) based on root transformed zooplankton abundance

Selected variables	Pseudo-F	P-value	Variation (%)	Cumulative (%)
IFDs	9.8	0.001	34.1	34.1
Chl_10	4.4	0.007	12.9	47.0

The best model of variables was selected based on the Akaike information criterion (AICc) for all locations. The pseudo–F, P–value were obtained by permutation ($n = 999$). IFDs was defined as the number of days after the SIC became less than 20%. Chl_10 was indicated > 10 µm chlorophyll a concentration

east–west differences in vertical distribution of *C. citer* at any of the developmental stages.

The developmental stage composition of the *C. citer* population varied spatially (Fig. 8a, b). The northernmost station was dominated by early–middle copepodite stages (CI–CIV), with very small contributions of adult stages (CVI_F and M). Early stages (CI–II) were present at high proportions in the northeast area, while the lowest proportion of these stages was found in the western area. Older stages (CV–CVI) were widely distributed throughout the study area, and the relative contributions of these stages were highest in the western area in 2017. In 2018, the population structure was similar to that observed in 2017, except at the southernmost station, which was dominated by early stages and adult females.

The best CCA model of relative stage composition was constrained by Temp200, Chl_10 and Chl_2, and explained 30% of the total inertia in the dataset ($p = 0.001$; Fig. 8c and Online Resource 4). The first axis, which accounted for the most variability (21%), was strongly correlated with average water temperature, which was inversely correlated with a large contribution of adult stages. Large proportions of early life stages were positively correlated with the Chl_2. Stations dominated by middle stages (CIII–CIV) had the highest Chl_10.

Discussion

Effects of interannual environmental variation on small zooplankton

Small copepods were numerically abundant at all stations, with particularly high abundances of *Oithona* spp., Oncaeidae, *C. citer*, *M. pygmaeus* and nauplii. These findings confirm a previous study on the oceanic zone of the Southern Ocean (Atkinson et al. 2012). Our results demonstrate a consistent latitudinal pattern across the 3 years. Spatial variations in abundance, with high abundances of small

copepods in the AZN and Polar Front (north of SACCF) and much lower abundances in the southern area of the AZS and coastal areas, are typically observed in East Antarctica (Dubischar et al. 2002; Hosie et al. 2014; Ojima et al. 2015; Takahashi et al. 2017, 2021; Makabe et al. 2017).

Despite this spatial variation, the zooplankton abundance in summer was highly variable among years. High abundance north of the SACCF reached 16,000 ind. m^{-3} in 2016 and 2018, which was four times greater than the abundance observed in 2017. The abundance in 2017 fell within the previously reported ranges obtained using 100 µm mesh nets (Dubischar et al. 2002; Ward et al. 2012a; Ojima et al. 2015). The abundance in the AZS was higher in 2016 than in the other 2 years and previous studies (Ojima et al. 2015; Takahashi et al. 2017; Makabe et al. 2017). The cluster analysis conducted in the present study supports these annual differences. The zooplankton community is strongly influenced by sea-ice dynamics, which often drives phytoplankton blooms, as indicated by the best model of zooplankton community composition. The sampling period was approximately 2 weeks later in 2016 than in the other 2 years, so the IFDs were longer in 2016. Previous studies have shown that zooplankton abundance increases with the phytoplankton bloom after sea-ice retreat, with a peak in fall (Hunt and Hosie 2006; Yang et al. 2011). During summer, blooms along with the sea-ice melt are the starting point for the recruitment of new generations of zooplankton and growth of these populations, which lead to increases in abundance (Ward et al. 2012a). Therefore, the observed differences in abundance between the 3 years are likely to be understood by the number of days between sea-ice retreat and sampling.

Zooplankton community structure is likely to be affected by phytoplankton in ice-edge blooms associated with the time of sea-ice retreat. This possibility was confirmed using the distLM procedure, which revealed that the variation in zooplankton community structure was correlated with the Chl_10 concentration and IFDs. To determine how the phytoplankton and ice-edge bloom changed after the sea-ice melted, we compared the monthly average chl a concentrations from November to January between the 3 years based on satellite ocean colour images of the Southern Ocean (Online Resource 5). Monthly mean chl a concentrations were highly variable among years in our research area. In January 2016, higher chl a concentrations were detected throughout the observation period across all sampling sites, while smaller blooms and low chl a concentrations were observed in 2017 and in the southern area in 2018. Ice-edge blooms are temporary events that disappear within several weeks (Arrigo et al. 2008). The high phytoplankton biomass (including released ice algae) provides a food resource for zooplankton (Kawall et al. 2001; Kohlbach et al. 2019). In this study, abundance and the egg production rate were positively correlated with chl a concentration for the most

Fig. 7 Horizontal and vertical distribution of developmental stages (CI–CVI) of *Ctenocalanus citer* in the upper 200 m. **a**: 110°E transect in 2017, **b**: 63.5°S transect in 2017 and **c**: 110°E transect in 2018. The histogram shows the percentages of total abundance for each developmental stage in three layers. The solid line denotes the log-transformed abundance of each developmental stage
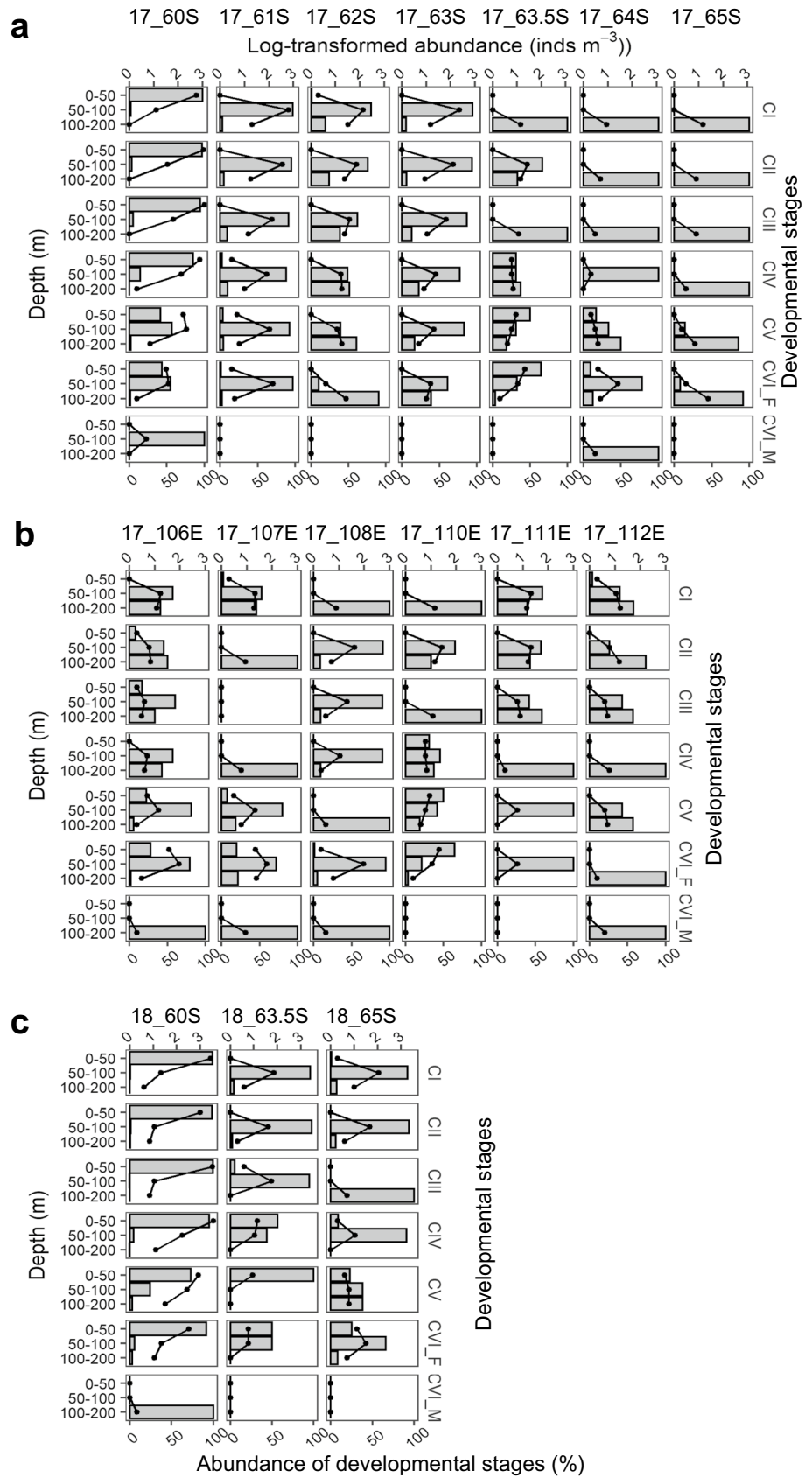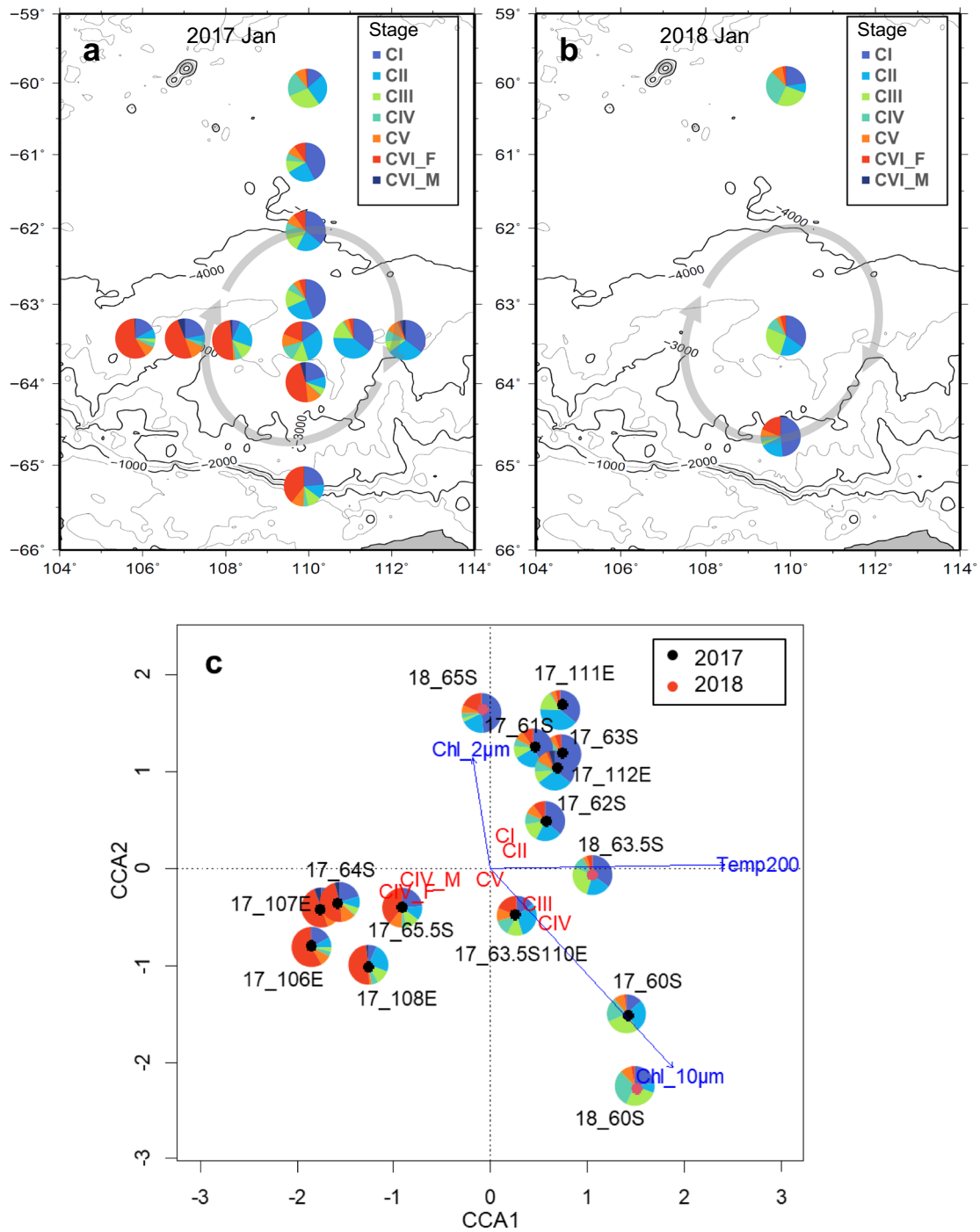
Fig. 8 Population structure (developmental stage composition) of *Ctenocalanus citer* at each location in January of 2017 and 2018 (**a**, **b**) and the results of canonical correspondence analysis (CCA) for relative developmental stage abundance in *C. citer* (**c**). In panels a and b, circulation arrows denote the Vincennes eddy. In panel c, the colour of the centre of each pie chart denotes sampling year (black: 2017; red: 2018). Arrows denote significant environmental factors with length representing the strength of the correlation to the ordination. Temp200 indicate average water temperature (0–200 m), Chl_10 indicate > 10 μm chl *a*. CI–CVI indicate the centroids for each developmental stage. (Color figure online)

dominant taxon, *Oithona* spp. (probably *O. similis*) (Ward and Hirst 2007; Pinkerton et al. 2020). In addition, Appendicularia was a major contributor to the dissimilarities in group A. In polar regions, Appendicularia respond rapidly to phytoplankton growth by altering the timing of their reproduction, resulting in peaks of abundance coincident with the ice-edge bloom (Acuña et al. 1999; Spinelli et al. 2018). Our results suggest that the abundance of small zooplankton increased owing to favourable feeding conditions and formed a consistent community throughout the SIZ in years with high primary production. However, the lower chl *a* concentrations observed in our study were associated with a lower abundance of zooplankton and with latitudinal variations in the zooplankton community (groups C and D). Most of the species contributing to the dissimilarity between the northern (group C) and southern (group D) communities were more abundant in the north, while *M. pygmaeus* was more abundant in the south. These species, except *M. pygmaeus*, are widely distributed in subantarctic and Antarctic waters (Atkinson and Sinclair 2000), and ubiquitous north and south of the SB-ACC (Hunt and Hosie 2006; Ojima et al. 2015). *M. pygmaeus* is an abundant species in Antarctic waters and is the most dominant species in the sea ice-covered western Weddell Sea during spring (Schnack-Schiel et al. 2008). The gradient in the distribution pattern of small zooplankton species is likely to be more enhanced during years with low food availability.

The abundance of small zooplankton and community structure varied annually, and were affected by the chl *a* concentration of the larger phytoplankton fraction associated with sea-ice retreat. The effects of hydrographic structure and local eddies were less apparent for small zooplankton. Small copepods have greater tolerance to changes in the physical environment, including frontal structures in the SIZ, than large zooplankton (Takahashi et al. 2017). These results suggest that small zooplankton respond to primary production through the food chain more quickly than large zooplankton. Therefore, regional effects of climate have the potential to affect the small zooplankton community in east Antarctica more rapidly than large zooplankton (Nicol et al. 2000).

Effects of environmental variations on the population structure of *Ctenocalanus citer*

In this study, the vertical distribution pattern and developmental stage of *C. citer* varied gradually with latitude. *C. citer* was distributed in shallower depths during both years at the northernmost station, with the intermediate stage dominating, while the vertical distribution of *C. citer* was deeper towards the south, with the adult stage dominating. In contrast, the east–west difference in the vertical distribution of *C. citer* was unclear, but the developmental stages differed,

with the younger stages dominating in the east and the adult stage dominating in the west.

The surface distribution of *C. citer* during summer has been reported in various regions of the Southern Ocean, such as the Scotia Sea (Atkinson and Sinclair 2000), the Lützow-Holm Bay region (Makabe et al. 2012; Takahashi et al. 2017) and the Polar Frontal Zone (Dubischar et al. 2002). *C. citer* migrates to the surface to graze on phytoplankton, which increases with sea-ice melting in the surface layer. Sea-ice melting proceeds from the north, suggesting that the time lag in melting is a potential factor causing the north–south difference in the vertical distribution. In addition, the vertical distribution of phytoplankton is likely to affect the vertical distribution patterns of *C. citer*. The depth of the SCM increased southwards during the study period. Thus, the spatial variation in the vertical distribution of *C. citer* during summer is also likely to depend on food availability in the water column.

The development of the *C. citer* population structure in the eastern Weddell Sea has previously been characterised (Schnack-Schiel and Hagen 1994; Schnack-Schiel 2001). The average population stage of *C. citer* is early copepodite (CI–CII) in late spring/summer, with rapid progression through the stages through winter. Although all developmental stages except adult males occur during all seasons, female gonads develop in late winter, coinciding with the occurrence of males. Females with mature gonads occur at high proportions in spring, which are maintained through autumn. *C. citer* exhibits seasonal migration, gradually ascending from November to February and spending the summer in the upper 100 m, where young generations are recruited (Schnack-Schiel and Mizdalski 1994).Therefore, analysis of the composition of developmental stages of copepods allows for the estimation of their population status.

The dominance of younger developmental stages (CI–CII) indicates the addition of new generations through reproduction. Likewise, the occurrence of middle stages (CIII–CVI) demonstrates a transition to adult stages in the population. Dominance of adult stages indicates a population just before or during the reproductive period. The developmental stage composition varied spatially. Middle stages dominated populations in the northern area, younger stages prevailed in the eastern area and adult stages predominated in the western area as well as in the southern area in 2017. These spatial differences in population structure are likely generated not only by oceanic frontal systems, such as the SACCF or SB-ACC, but also by the local east–west environmental gradient. Similar distribution patterns of copepod population structures were observed in Lützow-Holm Bay, East Antarctica (Makabe et al. 2017).

The CCA model revealed that the development of *C. citer* was controlled by average temperature and food availability. Water temperature in the epipelagic layer is negatively

correlated with the proportion of adult stages, suggesting that higher temperatures promote development in this species. This finding is consistent with previous studies, which showed that low temperatures resulted in longer egg hatching times and higher mortality of each stage for the marine copepod species (Ward and Shreeve 1998; Shreeve et al. 2002; Hirst and Bunker 2003). The water temperature differences between eastern and western areas along 63.5°S are likely driven by the Vincennes eddy circulation, which transports warm CDW poleward on the eastern side of the eddy and transports cold water equatorward on the western side (Mizobata et al. 2020). Thus, the environmental gradient formed by the cyclonic eddy affects the reproductive period of the dominant small copepod, *C. citer*, leading to an east–west difference in population structure. In addition, Mizobata et al. (2020) reported the presence of a cyclonic eddy train consisting of the Vincennes eddy, the Poinsett eddy and the Sabrina eddies in East Antarctica. These results indicate that local spatial differences in the population structure of copepods are common during summer in East Antarctica.

However, the population structure was slightly different in 2018, with no adults dominating anywhere. The dominant developmental stage was younger towards the south, which was probably related to the size composition of the phytoplankton. *C. citer* is predominantly herbivorous throughout the year (Hopkins and Torres 1988; Pasternak and Schnack-Schiel 2007). According to Pasternak and Schnack-Schiel (2007), and the largest size class of food items (> 25 µm) is rarely found in the guts of younger stages, and increases with *C. citer* stage. This finding is consistent with our CCA results, suggesting that it is difficult to assess the population dynamics of this species based on bulk chl *a* concentrations. The latitudinal changes in phytoplankton composition in the Indian sector of the Southern Ocean have been reported previously (Takao et al. 2014; Takahashi et al. 2022). In the study of Takahashi et al. (2022), which was conducted during the same voyage in 2018, the small diatom *Fragilariopsis cylindrus* was dominant at the sea-ice edge station, while larger diatoms, such as *Pseudo-nitzschia prolongatoides/subcurvata* and *Fragilariopsis kerguelensis*, were prevalent at the northern station. These latitudinal changes in phytoplankton species composition are a common feature in the SIZ of the Indian sector (Takahashi et al. 2017). These results suggest that shifts in phytoplankton composition (= latitudinal variation) in the SIZ after sea-ice melt are synchronous with the development of the *C. citer* population structure. This finding is also consistent with the summer surface distribution of *C. citer* (Schnack-Schiel and Mizdalski 1994; Schnack-Schiel 2001). It has been reported that feeding (Pasternak and Schnack-Schiel 2007), reproduction (Niehoff et al. 2002) and development of *C. citer* (Schnack-Schiel and Mizdalski 1994) are at least partially decoupled

from phytoplankton blooms, as they are observed outside the bloom period. Nevertheless, our results and those of a previous study in which *C. citer* abundance increased during the summer indicate that *C. citer* uses blooms efficiently for the growth of newly recruited populations during summer in the SIZ (Schnack-Schiel and Mizdalski 1994; Atkinson et al. 2012).

Conclusion

In this study, we examined the community structure and abundance of small zooplankton in SIZ off Vincennes Bay, East Antarctica, during summer (January 2016–2018). The small zooplankton community was highly variable among sampling periods in 2016, 2017 and 2018, and these patterns were likely driven by the abundance of large-sized phytoplankton and IFDs. Our results indicate that small zooplankton communities respond rapidly to changes in food availability after sea-ice melt. In contrast, the effect of hydrographic structure, such as fronts and local eddies, on small zooplankton community structure was unclear.

The population structure of *C. citer*, a key component of the small copepod community in the study area, was examined in relation to environmental factors. The developmental stage distribution pattern varied latitudinally and also between eastern and western areas. These spatial differences are likely to be driven by a local east–west environmental gradient. We suggest that the environmental gradient formed by cyclonic eddies influences the developmental period of *C. citer*, which in turn leads to the east–west difference in population structure. Local spatial variation in copepod population structure due to cyclonic eddies is likely to be common during summer in East Antarctica. The population structure of *C. citer* is also related to the spatiotemporal variation in the composition of primary producers after sea-ice melt, suggesting that the development of population structure is closely linked to the dynamics of the ice edge and phytoplankton blooms during summer.

Global warming is expected to cause changes in the Southern Ocean ecosystem as the extent and thickness of sea ice decreases (Arrigo and Thomas 2004; Constable et al. 2014). Our study demonstrated that small zooplankton species respond rapidly to these environmental changes in the Southern Ocean.

Declarations

References

Acuña JL, Deibel D, Bochdansky AB, Hatfield E (1999) In situ ingestion rates of appendicularian tunicates in the Northeast Water Polynya (NE Greenland). Mar Ecol Prog Ser 186:149–160. https://doi.org/10.3354/meps186149

Anderson, Marti, J., et al (2008) Permanova+ for Primer : guide to software and statisticl methods. PRIMER-E, Plymouth.

Aoki S, Rintoul SR, Hasumoto H et al (2006) Frontal positions and mixed layer evolution in the Seasonal Ice Zone along 140 E in 2001/02. Polar Biosci 20:1–20

Arrigo KR, Thomas DN (2004) Large scale importance of sea ice biology in the Southern Ocean. Antarct Sci 16:471–486. https://doi.org/10.1017/S0954102004002263

Arrigo KR, van Dijken GL, Bushinsky S (2008) Primary production in the southern ocean, 1997–2006. J Geophys Res. https://doi.org/10.1029/2007jc004551

Atkinson A (1996) Subantarctic copepods in an oceanic, low chlorophyll environment:ciliate predation, food selectivity and impact on prey populations. Mar Ecol Prog Ser 130:85–96. https://doi.org/10.3354/meps130085

Atkinson A (1998) Life cycle strategies of epipelagic copepods in the Southern Ocean. J Mar Syst 15:289–311. https://doi.org/10.1016/S0924-7963(97)00081-X

Atkinson A, Sinclair JD (2000) Zonal distribution and seasonal vertical migration of copepod assemblages in the Scotia Sea. Polar Biol 23:46–58. https://doi.org/10.1007/s003000050007

Atkinson A, Ward P, Hunt BPV et al (2012) An overview of Southern Ocean zooplankton data: abundance, biomass, feeding and functional relationships. Ccamlr Sci 19:171–218

Clarke K, Gorley R (2015) PRIMER v7: User manual/tutorial. Plymouth, UK: PRIMER-E Ltd

Comiso JC (1986) Characteristics of Arctic winter sea ice from satellite multispectral microwave observations. J Geophys Res 91:975. https://doi.org/10.1029/jc091ic01p00975

Comiso JC, Ackley SF, Gordon AL (1984) Antarctic sea ice microwave signatures and their correlation with in situ ice observations. J Geophys Res 89:662. https://doi.org/10.1029/jc089ic01p00662

Constable AJ, Melbourne-Thomas J, Corney SP et al (2014) Climate change and Southern Ocean ecosystems I: how changes in physical habitats directly affect marine biota. Glob Chang Biol 20:3004–3025. https://doi.org/10.1111/gcb.12623

Dubischar CD, Lopes RM, Bathmann UV (2002) High summer abundances of small pelagic copepods at the Antarctic Polar Front—implications for ecosystem dynamics. Deep Sea Res Part 2 Top Stud Oceanogr 49:3871–3887. https://doi.org/10.1016/S0967-0645(02)00115-7

Field JG, Clarke KR, Warwick RM (1982) A Practical strategy for analysing multispecies distribution patterns. Mar Ecol Prog Ser 8:37–52

Gallienne CP, Robins DB (2001) Is Oithona the most important copepod in the world's oceans? J Plankton Res 23:1421–1432. https://doi.org/10.1093/plankt/23.12.1421

Halfter S, Cavan EL, Swadling KM et al (2020) The role of zooplankton in establishing carbon export regimes in the southern ocean—a comparison of two representative case studies in the subantarctic region. Front Mar Sci 7:837. https://doi.org/10.3389/fmars.2020.567917

Hirst AG, Bunker AJ (2003) Growth of marine planktonic copepods: global rates and patterns in relation to chlorophylla, temperature, and body weight. Limnol Oceanogr 48:1988–2010. https://doi.org/10.4319/lo.2003.48.5.1988

Hopkins TL, Torres JJ (1988) The zooplankton community in the vicinity of the ice edge, western Weddell Sea, March 1986. Polar Biol 9:79–87. https://doi.org/10.1007/BF00442033

Hosie G, Mormède S, Kitchener J, et al (2014) 10.3 Near-surface zooplankton communities. In: Van de Putte A. P. Danis B. David B. Grant S. Gutt J. Held C. Hosie G. Huettmann F. Post A. Ropert-Coudert Y(Eds.)., Biogeographic Atlas of the Southern Ocean Scientific Committee on Antarctic Research, Cambridge (2014), pp. 422–430

Hunt BPV, Hosie GW (2005) Zonal structure of zooplankton communities in the Southern Ocean South of Australia: results from a 2150 km continuous plankton recorder transect. Deep Sea Res Part I 52:1241–1271

Hunt BPV, Hosie GW (2006) The seasonal succession of zooplankton in the Southern Ocean south of Australia, part I: the seasonal ice zone. Deep Sea Res Part I 53:1182–1202. https://doi.org/10.1016/j.dsr.2006.05.001

Hunt BPV, Pakhomov EA, Trotsenko BG (2007) The macrozooplankton of the Cosmonaut Sea, east Antarctica (30 E–60 E), 1987–1990. Deep Sea Res Part I 54:1042–1069

Kawall HG, Torres JJ, Geiger SP (2001) Effects of the ice-edge bloom and season on the metabolism of copepods in the Weddell Sea, Antarctica. Hydrobiologia 453:67–77. https://doi.org/10.1023/A:1013155614953

Kohlbach D, Lange BA, Graeve M et al (2019) Varying dependency of Antarctic euphausiids on ice algae- and phytoplankton-derived carbon sources during summer. Mar Biol 166:79. https://doi.org/10.1007/s00227-019-3527-z

Makabe R, Tanimura A, Fukuchi M (2012) Comparison of mesh size effects on mesozooplankton collection efficiency in the Southern Ocean. J Plankton Res 432:436. https://doi.org/10.1093/plankt/fbs014

Makabe R, Tanimura A, Tamura T et al (2017) Meso-zooplankton abundance and spatial distribution off Lützow-Holm Bay during austral summer 2007–2008. Polar Sci 12:25–33. https://doi.org/10.1016/j.polar.2016.09.002

Makabe R, Takao S, Takahashi KT, Odate T (2019) Chlorophyll a and macro-nutrient concentrations and photosynthetically active radiation during the training vessel Umitaka-maru cruises of the 58th

Japanese Antarctic Research Expedition in January 2017. Polar Data J 3:46–58. https://doi.org/10.20575/00000009

Makabe R, Takao S, Takahashi KT, Odate T (2020) Chlorophyll a and macro-nutrient concentrations and photosynthetically active radiation during the training vessel Umitaka-maru cruise of the 59th Japanese Antarctic Research Expedition in January 2018. Polar Data J 4:121–123

Massom RA, Stammerjohn SE (2010) Antarctic sea ice change and variability—physical and ecological implications. Polar Sci 4:149–186. https://doi.org/10.1016/j.polar.2010.05.001

Mizobata K, Shimada K, Aoki S, Kitade Y (2020) The cyclonic eddy train in the Indian ocean sector of the southern ocean as revealed by satellite radar altimeters and in situ measurements. J Geophys Res C: Oceans. https://doi.org/10.1029/2019jc015994

Montes-Hugo M, Doney SC, Ducklow HW et al (2009) Recent changes in phytoplankton communities associated with rapid regional climate change along the western Antarctic Peninsula. Science 323:1470–1473. https://doi.org/10.1126/science.1164533

Motoda S (1959) Device of simple plankton apparatus. Mem Fac Fish Hokkaido Univ 7:73–94

Nicol S, Pauly T, Bindoff NL et al (2000) Ocean circulation off east Antarctica affects ecosystem structure and sea-ice extent. Nature 406:504–507. https://doi.org/10.1038/35020053

Nicol S, Raymond B (2012) Pelagic ecosystems in the waters off east Antarctica (30° E-150° E). In: Antarctic Ecosystems. Wiley, Chichester, pp 243–254

Niehoff B, Schnack-Schiel S, Cornils A, Brichta M (2002) Reproductive activity of two dominant Antarctic copepod species, Metridia gerlachei and Ctenocalanus citer, in late autumn in the eastern Bellingshausen Sea. Polar Biol 25:583–590. https://doi.org/10.1007/s00300-002-0378-7

O'brien RM (2007) A caution regarding rules of thumb for variance inflation factors. Qual Quant 41:673–690. https://doi.org/10.1007/s11135-006-9018-6

Ojima M, Takahashi KT, Tanimura A et al (2015) Spatial distribution of micro- and meso-zooplankton in the seasonal ice zone of east Antarctica during 1983–1995. Polar Sci 9:319–326. https://doi.org/10.1016/j.polar.2015.05.002

Oksanen J, Blanchet FG, Friendly M, et al (2019) Vegan: Community Ecology Package. Software http://CRAN.Rproject.org/package=vegan

Orsi AH, Whitworth T, Nowlin WD (1995) On the meridional extent and fronts of the Antarctic Circumpolar Current. Deep Sea Res Part I 42:641–673. https://doi.org/10.1016/0967-0637(95)00021-W

Pansera M, Granata A, Guglielmo L et al (2014) How does mesh-size selection reshape the description of zooplankton community structure in coastal lakes? Estuar Coast Shelf Sci 151:221–235. https://doi.org/10.1016/j.ecss.2014.10.015

Pasternak AF, Schnack-Schiel SB (2007) Feeding of Ctenocalanus citer in the eastern Weddell Sea: low in summer and spring, high in autumn and winter. Polar Biol 30:493–501. https://doi.org/10.1007/s00300-006-0208-4

Pinkerton MH, Décima M, Kitchener JA et al (2020) Zooplankton in the Southern Ocean from the continuous plankton recorder: Distributions and long-term change. Deep Sea Res Part I 162:103303. https://doi.org/10.1016/j.dsr.2020.103303

R Core Team (2020) R: A Language and Environment for Statistical Computing. R Foundation for Statistical Computing, Vienna, Austria

Rohr T, Long MC, Kavanaugh MT et al (2017) Variability in the mechanisms controlling Southern Ocean phytoplankton bloom phenology in an ocean model and satellite observations. Global Biogeochem Cycles 31:922–940. https://doi.org/10.1002/2016gb005615

Schnack-Schiel SB, Hagen W (1994) Life cycle strategies and seasonal variations in distribution and population structure of four dominant calanoid copepod species in the eastern Weddell Sea, Antarctica. J Plankton Res 16:1543–1566. https://doi.org/10.1093/plankt/16.11.1543

Schnack-Schiel SB, Mizdalski E (1994) Seasonal variations in distribution and population structure of *Microcalanus pygmaeus* and *Ctenocalanus citer* (Copepoda: Calanoida) in the eastern Weddell Sea, Antarctica. Mar Biol 119:357–366. https://doi.org/10.1007/BF00347532

Schnack-Schiel SB, Michels J, Mizdalski E et al (2008) Composition and community structure of zooplankton in the sea ice-covered western Weddell Sea in spring 2004—with emphasis on calanoid copepods. Deep Sea Res Part 2 Top Stud Oceanogr 55:1040–1055. https://doi.org/10.1016/j.dsr2.2007.12.013

Schnack-Schiel SB (2001) Aspects of the study of the life cycles of Antarctic copepods. In: Lopes RM, Reid JW, Rocha CEF (eds.) Copepoda: Developments in Ecology, Biology and Systematics: Proceedings of the Seventh International Conference on Copepoda, held in Curitiba, Brazil, 25–31 July 1999. Springer Netherlands, Dordrecht, p 9–24

Shimada K, Makabe R, Takao S, Odate T (2020) Physical and chemical oceanographic data during Umitaka-maru cruise of the 58th Japanese Antarctic Research Expedition in January 2017. Polar Data J 4:1–29

Shreeve RS, Ward P, Whitehouse MJ (2002) Copepod growth and development around South Georgia: relationships with temperature, food and krill. Mar Ecol Prog Ser 233:169–183. https://doi.org/10.3354/meps233169

Smetacek V, Assmy P, Henjes J (2004) The role of grazing in structuring Southern Ocean pelagic ecosystems and biogeochemical cycles. Cambridge 16:541–558

Sokolov S, Rintoul SR (2002) Structure of Southern Ocean fronts at 140°E. J Mar Syst 37:151–184. https://doi.org/10.1016/S0924-7963(02)00200-2

Spinelli ML, Franzosi C, Olguin Salinas H et al (2018) Appendicularians and copepods from Scotia Bay (Laurie island, South Orkney, Antarctica): fluctuations in community structure and diversity in two contrasting, consecutive summers. Polar Biol 41:663–678. https://doi.org/10.1007/s00300-017-2227-8

Stammerjohn S, Massom R, Rind D, Martinson D (2012) Regions of rapid sea ice change: an inter-hemispheric seasonal comparison. Geophys Res Lett. https://doi.org/10.1029/2012gl050874

Stevens CJ, Pakhomov EA, Robinson KV, Hall JA (2015) Mesozooplankton biomass, abundance and community composition in the Ross Sea and the Pacific sector of the Southern Ocean. Polar Biol 38:275–286. https://doi.org/10.1007/s00300-014-1583-x

Suzuki R, Ishimaru T (1990) An improved method for the determination of phytoplankton chlorophyll using N, N-dimethylformamide. J Oceanogr Soc Japan 46:190–194. https://doi.org/10.1007/BF02125580

Tachibana A, Watanabe Y, Moteki M et al (2017) Community structure of copepods in the oceanic and neritic waters off Adélie and George V Land, East Antarctica, during the austral summer of 2008. Polar Sci 12:34–45. https://doi.org/10.1016/j.polar.2016.06.007

Takahashi KT, Ojima M, Tanimura A et al (2017) The vertical distribution and abundance of copepod nauplii and other micro- and mesozooplankton in the seasonal ice zone of Lützow-Holm Bay during austral summer 2009. Polar Biol 40:79–93. https://doi.org/10.1007/s00300-016-1925-y

Takahashi KT, Takamura TR, Odate T (2021) Zooplankton communities along a Southern Ocean monitoring transect at 110° E from three CPR surveys (Dec 2014, Jan 2015, Mar 2015). Polar Biol. https://doi.org/10.1007/s00300-021-02862-z

Takahashi KD, Makabe R, Takao S et al (2022) Phytoplankton and ice-algal communities in the seasonal ice zone during January (Southern Ocean, Indian sector). J Oceanogr 78:409–424. https://doi.org/10.1007/s10872-022-00649-2

Takao S, Hirawake T, Hashida G et al (2014) Phytoplankton community composition and photosynthetic physiology in the Australian sector of the Southern Ocean during the austral summer of 2010/2011. Polar Biol 37:1563–1578. https://doi.org/10.1007/s00300-014-1542-6

Tanimura A, Kawaguchi S, Oka N et al (2008) Abundance and grazing impacts of krill, salps and copepods along the 140\^ oE meridian in the Southern Ocean during summer. Antarct Sci 20:365

Turner JT (2004) The importance of small planktonic copepods and their roles in pelagic marine food webs. Zool Stud 43:255–266

Turner JT (1984) The feeding ecology of some zooplankters that are important prey items of larval fish. NOAA Technical Report NMFS 7

Ward P, Shreeve R (1998) Egg hatching times of Antarctic copepods. Polar Biol 19:142–144. https://doi.org/10.1007/s003000050225

Ward P, Hirst AG (2007) Oithona similis in a high latitude ecosystem: abundance, distribution and temperature limitation of fecundity rates in a sac spawning copepod. Mar Biol 151:1099–1110. https://doi.org/10.1007/s00227-006-0548-1

Ward P, Atkinson A, Tarling G (2012) Mesozooplankton community structure and variability in the Scotia Sea: A seasonal comparison. Deep Sea Res Part 2 Top Stud Oceanogr 59–60:78–92. https://doi.org/10.1016/j.dsr2.2011.07.004

Ward P, Atkinson A, Venables HJ et al (2012) Food web structure and bioregions in the Scotia Sea: A seasonal synthesis. Deep Sea Res Part 2 Top Stud Oceanogr 59–60:253–266. https://doi.org/10.1016/j.dsr2.2011.08.005

Yang G, Li C, Sun S (2011) Inter-annual variation in summer zooplankton community structure in Prydz Bay, Antarctica, from 1999 to 2006. Polar Biol 34:921–932. https://doi.org/10.1007/s00300-010-0948-z